Journal of Materials Chemistry A

Accepted Manuscript

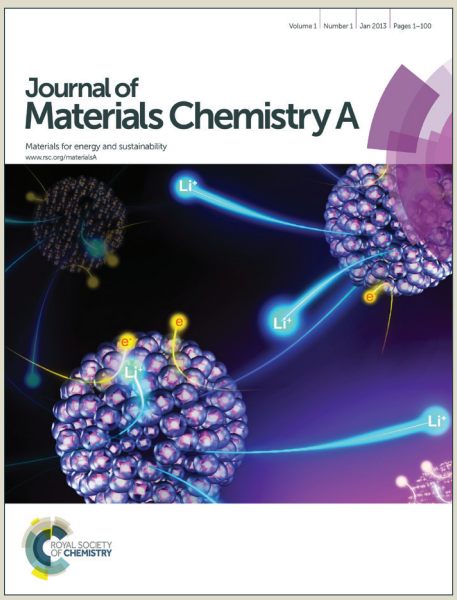

ROYAL SOCIETY OF CHEMISTRY

www.rsc.org/materialsA

Journal of Material Chemistry A

Cite this: DOI: 10.1039/c0xx00000x

www.rsc.org/xxxxxx

PAPER

Preparation and Properties of a Novel Form-stable Phase Change Material Based on Gelator

Dang Wu, Wen Wen, *Sheng Chen and *Hailiang Zhang***

Received (in XXX, XXX) Xth XXXXXXXXX 20XX, Accepted Xth XXXXXXXXX 20XX

DOI: 10.1039/b000000x

A series of gelators (Gm, m is the length of alkyl tails, m = 2, 4, 6, 8, 10, 12, 14, 16 and 18) containing 4, 4′-diaminodiphenylmethane moieties were synthesized. The chemical structures of Gm were confirmed by ^{1}H NMR and MS. The form-stable phase change materials (PCMs) were prepared by introducing Gm into paraffin. The minimum gelation concentration (MGC) and gel-to-sol transition temperature (T_{GS}) properties were tested by "tube-testing method". It found that Gm (m = 2, 4, 6) was insoluble in paraffin, while MGC and T_{GS} of Gm (m = 8, 10, 12, 14, 16, 18) increased with the increase of alkyl chain. The structure and morphology of PCMs were systematically investigated by FT-IR, POM, 1D WXAD and SEM. Experimental results revealed that paraffin was restricted because the gelators could self-assemble into three-dimensional netted structural, leading to form the shape-stable PCMs without leakage even above its melting point. The thermal properties were studied by DSC. The research showed that the G18/paraffin FSPCMs exhibited excellent thermal stability and high heat storage density. The shape stability of G18/paraffin was discussed by rheological measurement, indicating that solid ↔ hard gel ↔ soft gel ↔ liquid was observed with the increase of temperature. Through researching, this work is useful in the comprehensive academic research and industrial application of PCMs.

Introduction

Thermal energy storage application has gained great attention in recent years because of energy crisis, the rising demand of energy consumption, high cost of fossil fuels and the accompanied environmental problems. Thermal energy storage as an effective use of thermal energy has been applied in diverse areas, such as building heating/cooling systems, solar energy collectors, power and industrial waste heat recovery.[1-3]

Phase change materials (PCMs) can store and release large amounts of energy during phase change process, the application of which has been investigated as one of prospective techniques of storing thermal energy in decades.[4-7] PCMs can be classified into two major categories: inorganic compounds and organic compounds. Inorganic PCMs include salt hydrates, salts, metals and alloys, whereas organic PCMs are comprised of paraffin, fatty acids/esters and polyalcohols.[8] According to phase change pattern, practically applied PCMs can be classified into solid-solid PCMs and solid-liquid PCMs. For the solid-solid PCMs, the advantages are that there is no liquid or gas generated, so accordingly no recipient is needed to seal them in, during the solid-solid phase transitions. However, the small latent heats and the super-cooling limit their application.[9-11] To our best knowledge, numerous of solid-liquid PCMs has been studied for decades, such as, fatty acid, fatty alcohol, paraffin wax, polyethylene glycol (PEG), due to their superior properties, which have proper melting temperature range, high heat storage capacity, good thermal stability, little or no super-cooling, low vapor pressure, no or less volume change during solid-liquid phase transition, non-toxicity, self-nucleating behaviour, good thermal and chemical stability after long-term utility period, low cost, commercially produced and so on.[12-34] However, solid-liquid PCMs have to be placed in specially designed devices/containers during application to prevent the leakage in their solid-liquid phase transition process, which results in extra thermal resistance and cost.[35-37]

In order to solve the above problems, a wide class of form-stable phase change materials (FSPCMs) which are composite materials that contain solid-liquid PCM (thermal energy storage material) and supporting material (maintains the solid shape of the FSPCMs) has aroused widely interest from researchers in recent years.[38] The main research of FSPCMs focus on finding efficiency supporting materials which can remain the composite material solid and stable without liquid leakage even above the melting temperature of the PCM. There are several methods to prepare FSPCMs: (1) Encapsulating solid-liquid PCMs into a polymeric structure by blending or situ polymerization. There are

Key Laboratory of Polymeric Materials and Application Technology of Hunan Province, Key Laboratory of Advanced Functional Polymer Materials of Colleges, Universities of Hunan Province, College of Chemistry, Xiangtan University, Xiangtan 411105, Hunan Province, China. Email: zhl1965@xtu.edu.cn

† Electronic Supplementary Information (ESI) available. See DOI: 10.1039/c0xx00000x

many supporting polymers to be used, such as polymethyl methacrylate (PMMA),[39-41] high-density polyethylene (HDPE),[42-43] low density polyethylene (LDPE),[44] polypropylene,[45] etc. (2) Absorbing solid-liquid PCMs into porous materials like expanded perlite,[46-47] vermiculite,[48] diatomite,[49] expanded graphite.[50] (3) Grafting solid-liquid PCMs onto the skeleton of high melting temperature polymers.[51-53] (4) Microencapsulating solid-liquid PCMs with different shells.[54-56] (5) Encapsulating solid-liquid PCMs into SiO_2 net structure.[57-59] Although these methods for FSPCMs have successfully prevented the leakage of solid-liquid PCMs, the application range is still restricted due to some drawbacks: (1) The latent heat is reduced by introducing of large amount of supporting materials. (2) Some of FSPCMs cannot be processed repeatedly once prepared. (3) The complex process of preparation will bring the increase of cost.

When analyzing the shortcomings of FSPCMs mentioned above, it's obvious that the introduction of supporting materials will lead to the reducing of the energy storage density, so we are interested in finding a new kind of supporting materials, which can make the PCMs remain shape stable at low concentration, high latent heat and low cost .

Low molecular mass organic gelators (LMOGs) are organic molecules capable of immobilizing organic or aqueous solvents when a solution containing a small amount of LMOG is cooled below its gelation temperature.[60] The resultant low-molecular-weight gels (LMWGs) present the viscoelastic solid-like state because the organic or aqueous solvents were restricted by complex three-dimensional networks self-assembled by LMOGs. Accordingly, the organic or aqueous solvents can be replaced by solid-liquid PCMs, and the three-dimensional networks self-assembled by LMOGs are assumed to support the solid-liquid PCMs as they undergo solid-liquid transition. Recently, Zhang and Tian has researched the properties of gelatinous shape-stabilized PCMs by impregnating 1, 3:2, 4-di-(4-methyl) benzylidene sorbitol (MDBS) or 1, 3:2, 4-di-(3, 4-dimethyl) benzylidene sorbitol (DMDBS) into paraffin and 1-tetradecanol,[61-62] which may open a new way to prepare the form-stable PCMs.

In this paper, we synthesized a series of gelators (Gm, m is the length of alkyl tails, m = 2, 4, 6, 8, 10, 12, 14, 16 and 18) based on 4, 4′-diaminodiphenyl-methane with amide moieties, which could gel organic solvents with low concentration (typically < 2 wt%) through hydrogen-bonding and π - π stacking interactions.[63] The chemical structures of Gm are shown in Chart 1. Paraffin was used as latent heat material due to its high heat of fusion, proper range of phase change temperatures, chemical resistance, commercial availability, and low cost. The gelator/paraffin composites (Gm/paraffin) were prepared and the thermal properties and thermal stability were investigated. Since there were few reports about using gelators for supporting typical solid-liquid PCMs, this work widened the range of application of gelators as well as offered a promising FSPCMs with high thermal storage density and thermal reversibility.

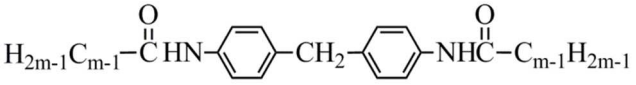

m = 2, 4, 6, 8, 10, 12, 14, 16, 18

Chart 1 Chemical structures of Gm.

Experimental

Materials

Paraffin was provided by Shanghai Huashen Recover Equipment Co., Ltd. Gelators (Gm, m = 2, 4, 6, 8, 10, 12, 14, 16 and 18) were synthesized according to Ref. 63. The composite PCMs were prepared by mixing paraffin and Gm, heating to solution states, followed by cooling to room temperature. All other compounds were analytical grade and were used without any further treatment.

Synthesis of gelators

According to the literature,[63] the gelators (Gm, m = 2, 4, 6, 8, 10, 12, 14, 16 and 18) containing 4, 4′-diaminodiphenylmethane moieties were easily synthesized (see supporting information). The synthetic routes of Gm were shown in Scheme 1.

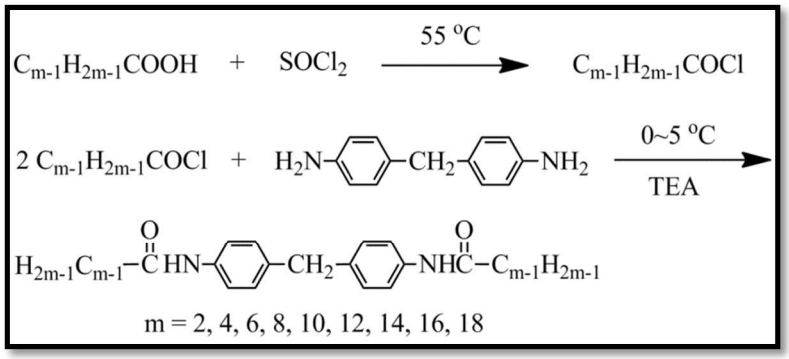

Scheme 1 Synthesis route of Gm.

Preparation of Gm/PCMs

The mixture of gelator and paraffin were sealed in a test tube, then heated at 160 °C until a transparent solution was formed. For example, the preparation of 2 wt% G18/paraffin was described as follows: 0.02 g (0.113 mmol) G18 was added into 0.98 g paraffin in a test tube to form a suspension. After being heated in an oil bath at about 160 °C, the mixture gradually turned into a transparent solution. Then, the tube was cooled at room temperature (25 °C) until a white gel was formed (see Fig.3). All the other gels were prepared via the similar method.

Instruments and measurements

^{1}H NMR measurements. All NMR measurements were performed on a Bruker ARX400 MHz spectrometer using with $CDCl_3$ as solvent, tetramethylsilane (TMS) as the internal standard at ambient temperature. The chemical shifts were reported on the ppm scale.

Minimum gelation concentration (MGC) and gel-to-sol transition temperature (T_{GS}) measurements. The MGC and T_{GS} properties were tested by a "tube-testing method"[64]: A weighted gelator was mixed with paraffin in a test tube (the samples were weighed in at 1g in total) with a screw cap (inside diameter was 14 mm), heated until the gelator was dissolved. The resulting solution was cooled at 25 ^oC for 2 h, and then put into oil-bath whose temperature was above melting temperature of solid-liquid PCMs. When upon inversion of the test tube no fluid ran down the walls of the tube, we judged it "successful gelation". The minimum concentration of gelator necessary for gelation is MGC, the unit of MGC is wt%. The temperature that gel turn into sol is T_{GS}.

Fourier transform infrared (FT-IR) analysis. Infrared spectrogram of each specimen was obtained in transmittance mode using a Nicolet Nexus 6700 FT-IR spectrophotometer with a 1 cm resolution in 32 scans collect. The samples were scanned in the range of 500 - 4000 cm^{-1} using KBr pellets.

Polarized optical microscope (POM) observation. Polarized optical microscope observation was carried out using a Leica DMLM-P microscope equipped with a Mettler FP82 hot stage and a digital camera. Photographs were taken by a digital camera at short intervals of time.

Wide angle X-ray diffraction (WAXD) analysis. One-dimensional wide-angle X-ray diffraction (1D WAXD) experiments were performed on a BRUKER AXS D8 Advance diffractometer with a 40 kV FL tubes as the X-ray source (Cu Kα) and the LYNXEYE_XE detector. Background scattering was recorded and subtracted from the sample patterns.

Scanning election microscope (SEM) observation. To investigate the nature of microstructures and morphologies, a SEM sample was prepared by immersing the PCMs gels in petroleum ether to extract the PCMs for 5 h followed by drying at room temperature,[63] and then the specimens were examined under A JEOL JSM-6610 SEM.

Differential scanning calorimetry (DSC) measurement. DSC traces of the polymer were obtained using a TA Q10 DSC instrument. The temperature and heat flow were calibrated using standard materials (indium and zinc) at a cooling and heating rates of 5 ^oC min^{-1}. The sample with a typical mass of about 5 mg was encapsulated in sealed aluminum pans.

Rheology measurement. A Rheometrics ARES rheometer (TA ARES rheometer) was applied to measure the viscoelastic properties of the samples based on oscillatory shear and temperature. The experimental temperature was controlled using forced N_2 gas convection. Dynamic temperature ramp test were performed in the region of 30 ^oC to 160 ^oC at 2 ^oC min^{-1}, using a 25 mm diameter parallel-plate geometry with a frequency of 1 rad s^{-1} and a small strain amplitude. Isothermal frequency sweeps were made using the same setup at frequencies from 0.1 to 100 rad s^{-1}.

Results and discussion

Synthesis and characterization of gelators and composite Gm/PCMs

Gm were synthesized according to the method discussed in Ref. 63. The ^{1}H NMR spectra of G18 was shown in Fig.1. The MGC and T_{GS} test results of Gm/paraffin were shown in Fig.2. It found that, Gm (m = 2, 4, 6) were insoluble in paraffin, while paraffin can be gelated when introducing Gm (m = 8, 10, 12, 14, 16, 18) at a low mass fraction (below 3 wt%), and the MGC of Gm/paraffin decreased with the increase of alkyl chain of gelators (see Fig.2a). Moreover, G18 can even gelate paraffin at concentration of 0.5 wt%. This may result from the solvophilic interaction of long alkyl groups to increase the interaction between gelator and paraffin. Meantime, T_{GS} of Gm/paraffin at a certain mass fraction (3 wt%) decreased with the increase of alkyl chain of gelators (see Fig.2b). This can partly be explained by the difference in melting points of the pure Gm according to the Schröder-van Laar relation,[65] which is that the T_{GS} is related to the melting point of the pure gelator.[66] It's worth mentioning that, the gelation process is reversible (see Fig.3). Compared to Gm/paraffin (m = 8, 10, 12, 14, 16), G18/paraffin showed better compatibility, lower MGC and excellent thermal stability, Thus, it is necessary to discuss G18/paraffin in details as the example in the whole paper.

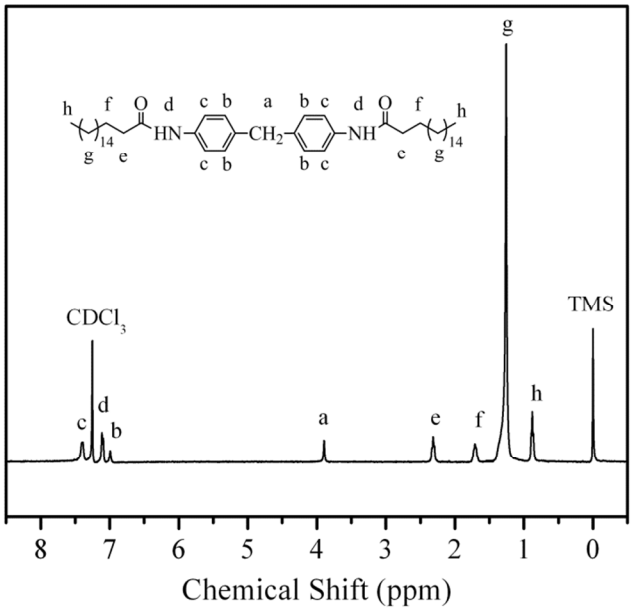

Fig.1 ^{1}H NMR spectrum of G18 in $CDCl_3$.

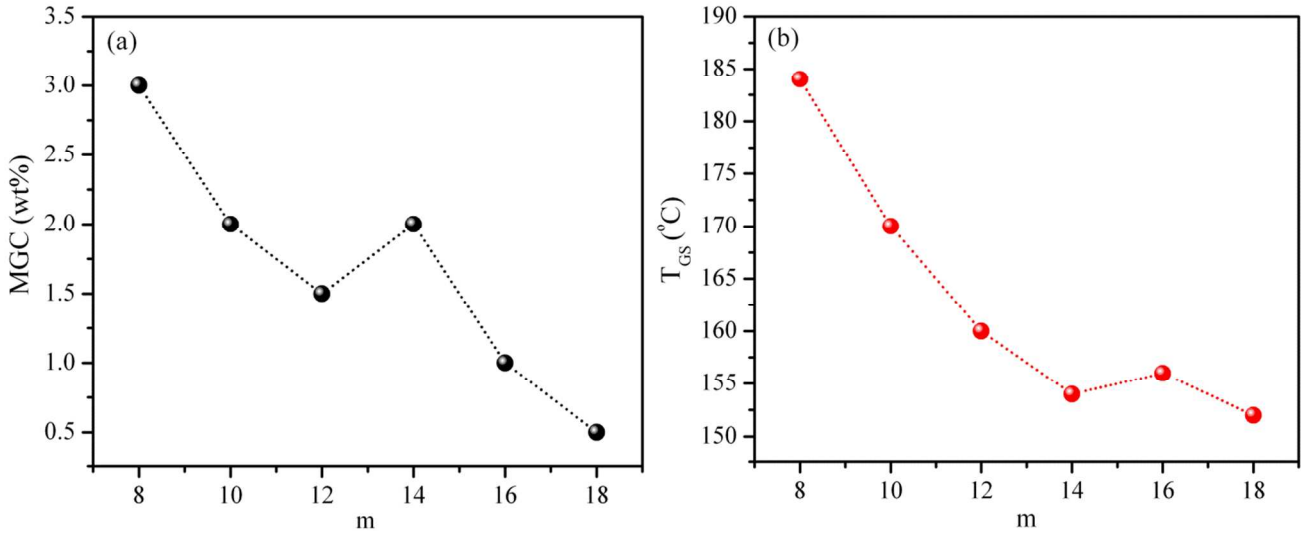

Fig.2 (a) MGC of Gm in paraffin; (b) T_{GS} of 3 wt% Gm/paraffin by a tube-testing method.

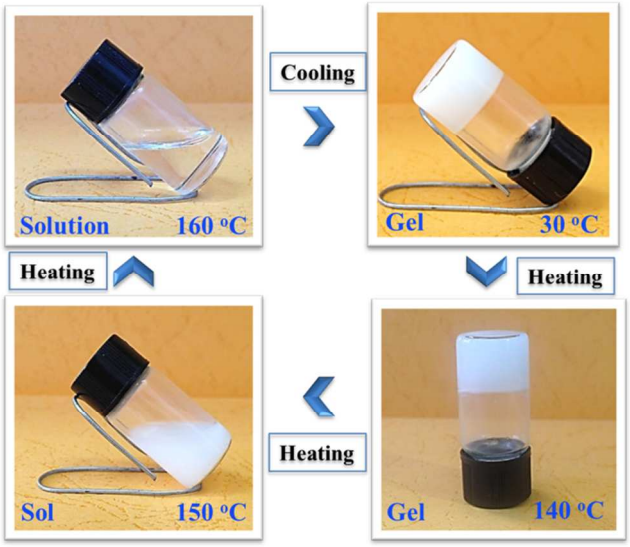

Fig.3 Photographs of gelation result of 3 wt% G18/paraffin FSPCM at different temperature.

Structure characterization of the form-stable Gm/PCMs

The FT-IR spectra of the neat G18, paraffin, 3 wt% G18/paraffin were shown in Fig.4. It was observed that IR peaks of H-N and C=O moieties appeared at about 3300 and 1659 cm^{-1}, respectively. The similar spectral positions were observed both in neat powders of the G18 and G18/paraffin composite as shown in Fig.4. It could be inferred that hydrogen bonding was similar in the two phases. However, the H-N stretching vibration band in the gel state was broader than that of neat state for the disorder in the gel fibrils. In the spectrum of G18 (Fig.4a), it was observed that IR peaks of H-N and C=O moieties appeared at about 3300 and 1659 cm^{-1}, respectively. In the spectrum of paraffin (Fig.4b) the peak at 2917 cm^{-1} signifies the symmetrical stretching vibration of its -CH_3 group, the peak at 2849 cm^{-1} represents the symmetrical stretching vibration of its -CH_2 group. The peaks at around 1463 cm^{-1} belong to the deformation vibration of -CH_2 and -CH_3, and the peak at 719 cm^{-1} represents the rocking vibration of -CH_2. In the spectrum of composite G18/paraffin (Fig.4c), the same peaks as G18 and paraffin still existed, and no significant new peak was observed, indicating that the composite G18/paraffin was only a physical interaction between paraffin and G18 and there was no chemical reaction to occur between them.

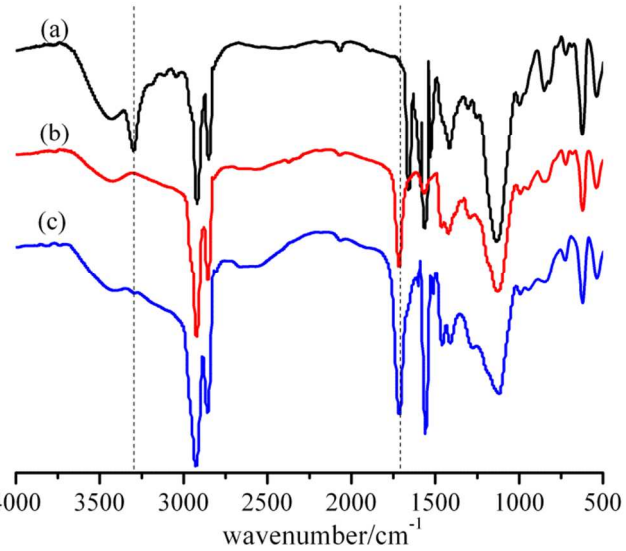

Fig.4 IR spectra of (a) neat G18, (b) paraffin, (c) 3 wt% G18/paraffin.

Fig.5 shows the polarizing optical microscope (POM) micrographs of PCMs. As can been seen from Fig.5a to Fig.5b, no birefringence phenomenon was observed when the paraffin melted. Contrary to the neat paraffin, the G18/paraffin present birefringence phenomenon above the melting point of paraffin (T_m), as can be seen from Fig.5c to Fig.5d, showing that the G18 formed the order structure in the solid-liquid PCMs. Unlike the crystallization of neat G18 (Fig.S1), a number of crossed fiber-like aggregations were observed in G18/paraffin composite. Although the paraffin component melted totally above the T_m, no obvious flow of PCMs was observed from POM micrograph, and the birefringence phenomenon remained until the temperature get

to 150 °C, suggesting that the supporting of G18 gel network restricted the flow of melted paraffin, resulting in form-stable composite PCMs with good thermal stability. Moreover, there was no difference in crystal structure between neat paraffin and G18/paraffin (Fig.5a and Fig.5c), indicating that G18 has little effect on crystal structure of PCMs.

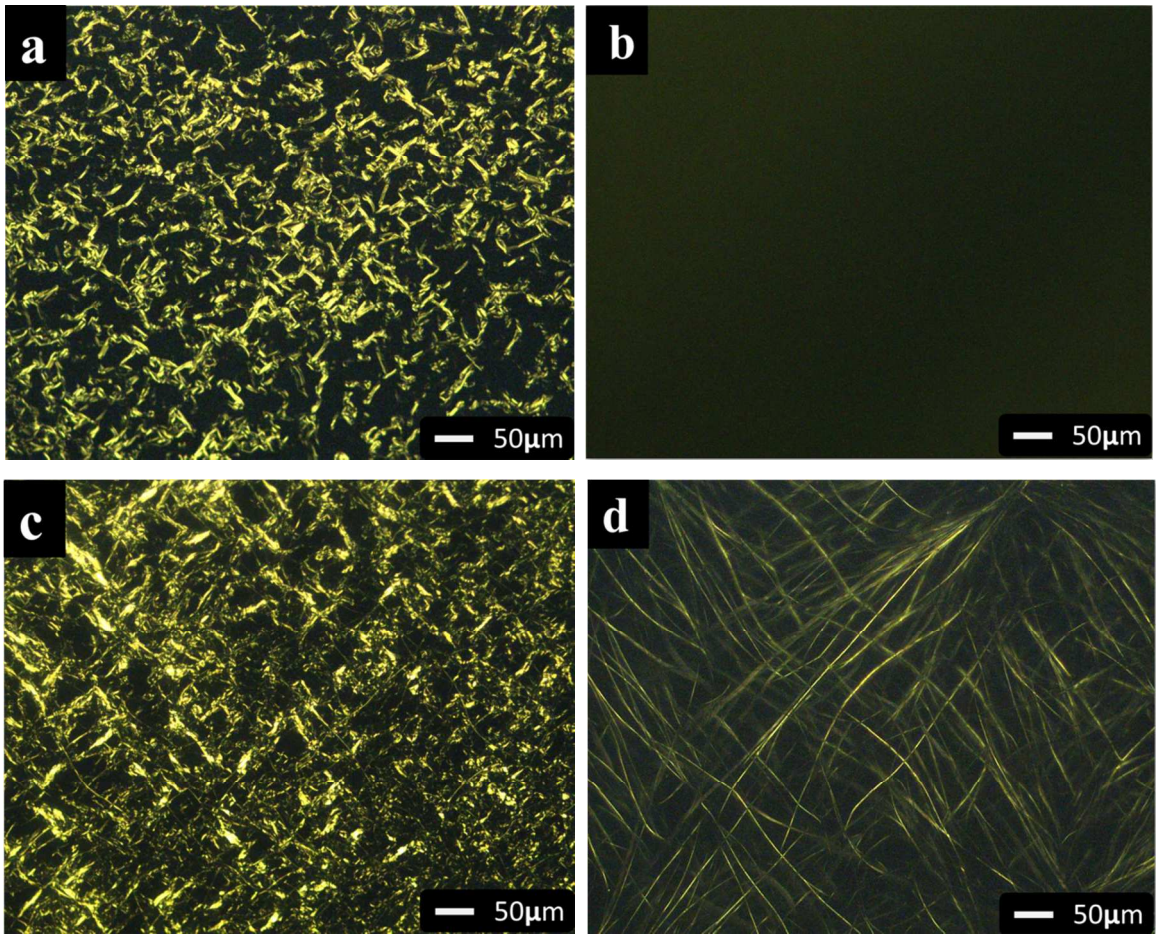

Fig.5 POM images (×200) of paraffin at 30 °C (a) and 70 °C (b); 3 wt% G18/paraffin at 30 °C (c) and 70 °C (d).

The results were further supported by 1D WAXD. The 1D WAXD patterns of the paraffin, G18 and different mass fractions of G18/paraffin composite PCMs were presented in Fig.6a. In the high 2θ region of 15 - 25°, the two peaks appeared at 21.3° and 23.7° for the paraffin and at 20.8° and 21.3° for the G18, indicating the formation of crystal. The 1D WAXD patterns of the composite PCMs contains all the diffraction peaks of paraffin, whereas the peak intensities were relatively reduced with the increase of concentration of G18. However, the peaks of G18 were covered by paraffin. The results suggested that the crystal structure of the G18/paraffin composite was not destroyed by G18. As shown in Fig.6b, the sharp peaks at 21.3° and 23.7° disappeared when heating to 60 °C, showing that the melting of paraffin in the G18/paraffin composite. The peaks at 20.8 ° and 21.3° didn't disappear until the temperature get to 150 °C, showing that G18 was dispersed in paraffin with an ordered structure, lead to the well supporting behavior for G18/paraffin. The results above were consistent with the POM results. Diffractograms of G18 in neat powder and xerogel by extracting the paraffin in low angle were shown in Fig.6c. The XRD pattern of the xerogel revealed that a similar structure was adopted by the aggregates of the gelators in the gel state. The obtained long Bragg distances (d) of the xerogel were 4.88, 1.60, 1.19 and 0.08nm (1, 1/3, 1/4, 1/6), respectively, which suggesting that G18 self-assembles into a lamellar structure,[67,68] the lamellar repeat was evaluated as 4.88 nm. The calculated van der Waals lengths (5.18 nm) of the fully extended G18 molecules calculated from Materials Studio 6.0 (Accelrys, Inc.) model were slightly longer than Bragg distances (d), which suggested that their long chains must be tilted with lamellar planes or interdigitated with each other.[69]

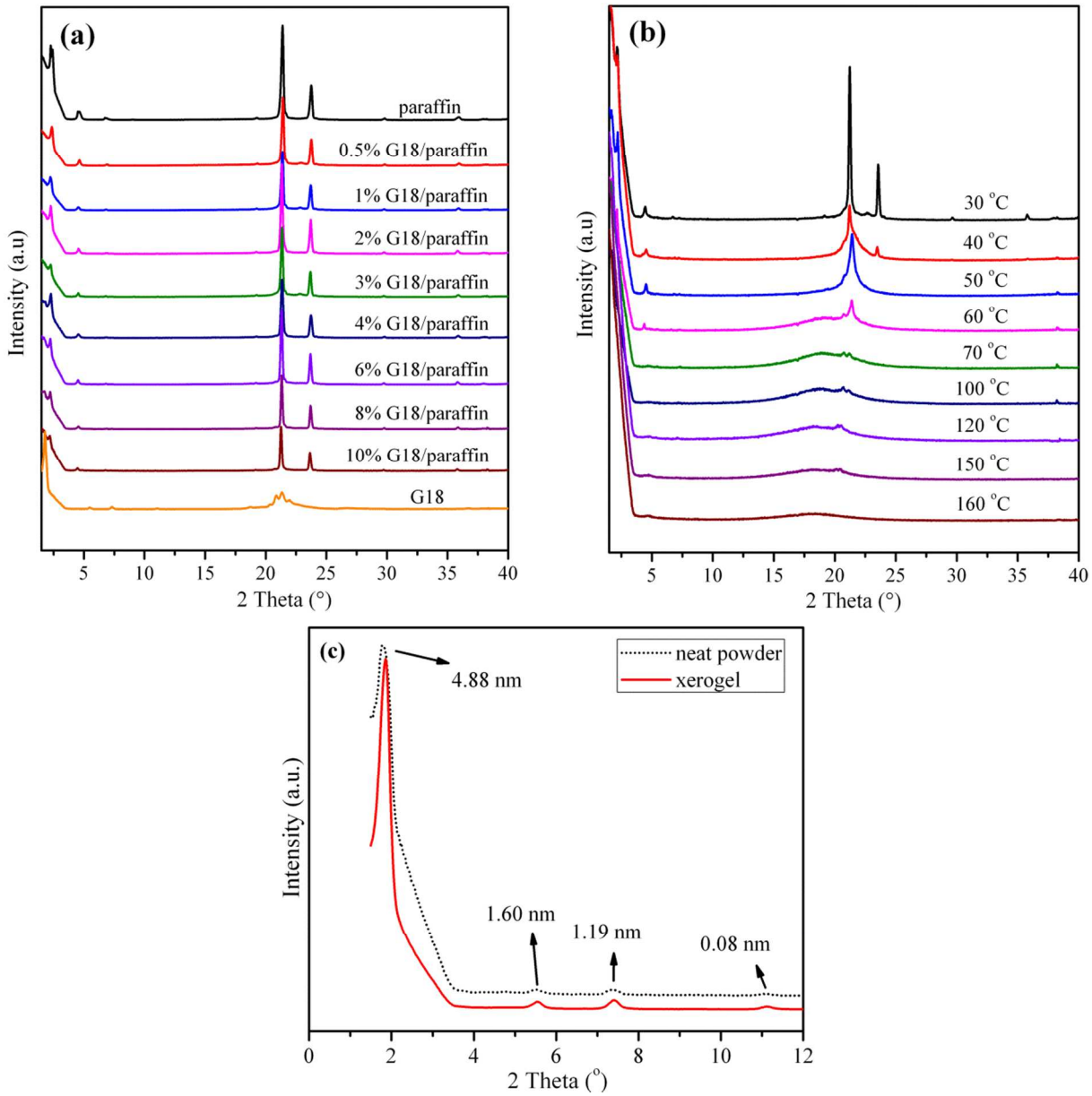

Fig.6 1D WAXD patterns of (a) paraffin, G18 and G18/paraffin at room temperature; (b) 10 wt% G18/paraffin during the heating process; (c) Diffractograms of G18 in neat powder and xerogel by extracting the paraffin.

The Fig.7a and b shows the SEM images of pure paraffin and G18/paraffin composite, respectively. Unlike the smooth and uniform surface of paraffin in Fig.7a, the dark and light regions were observed in G18/paraffin which represent the paraffin and G18, respectively. The paraffin was uniformly dispersed in the G18. The microstructures of the G18/paraffin xerogel prepared by removing the paraffin were further observed in Fig.7c and d. The three-dimensional network was constructed by ribbon-like microfibers and the average diameter of the ribbons was about 400 - 1000 nm. Meantime, both the density and diameter of the ribbons increased with the increase of the concentration of G18 (Fig.S2). In addition, the microstructures of the Gm/paraffin (m = 8, 10, 12, 14, 16) xerogel were observed in Fig.S3. Three-dimensional networks constructed by ribbon-like microfibers were also observed. The results indicating that Gm (m = 8, 10, 12, 14, 16) self-assembled into a similar network to G18 in paraffin. The dense entanglement of ribbons traps the solid-liquid PCMs, so even if the environmental temperature is above their melting point, the composite FSPCMs remain in the solid state.

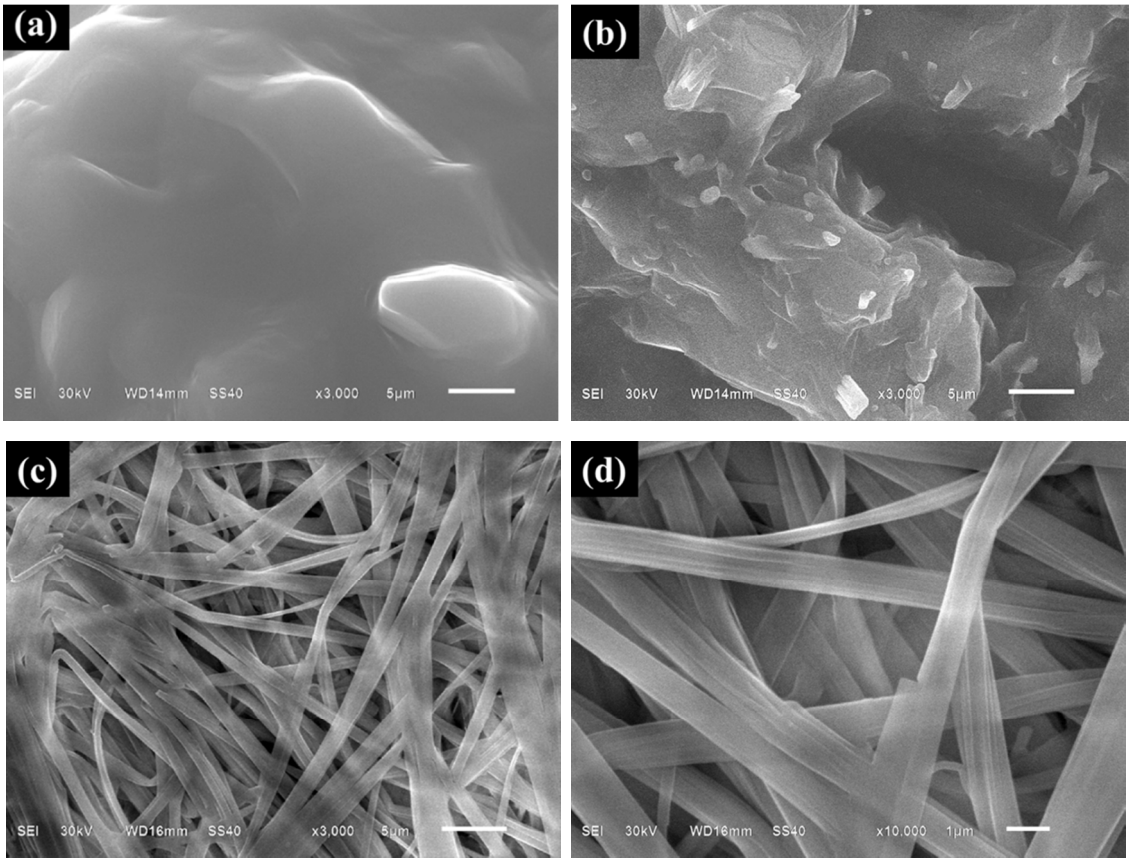

Fig.7 SEM images of (a) pure paraffin, (b) G18/paraffin composites, (c) and (d) xerogel of G18/paraffin composites at different magnifications. Scale bar = 5 μm for a, b and c, and 1 μm for (d), respectively.

Thermal properties of Gm/PCM composites

The heating and cooling DSC curves of the G18/paraffin composite PCM, pure paraffin and G18 are shown in Fig.8. From the figure, it can be seen that three peaks were detected in the G18/paraffin composite DSC curve. The first minor peak at about 39 °C should be attributed to the solid-solid phase transition of the paraffin and the second sharp peak at about 57 °C corresponding to the solid-liquid phase transition of the paraffin.[70] The third phase transition peak appeared at about 130 to 155 °C was well correlated to T_{GS} values obtained by the tube-testing method at the same gelator concentrations, showing a gel-sol transition.

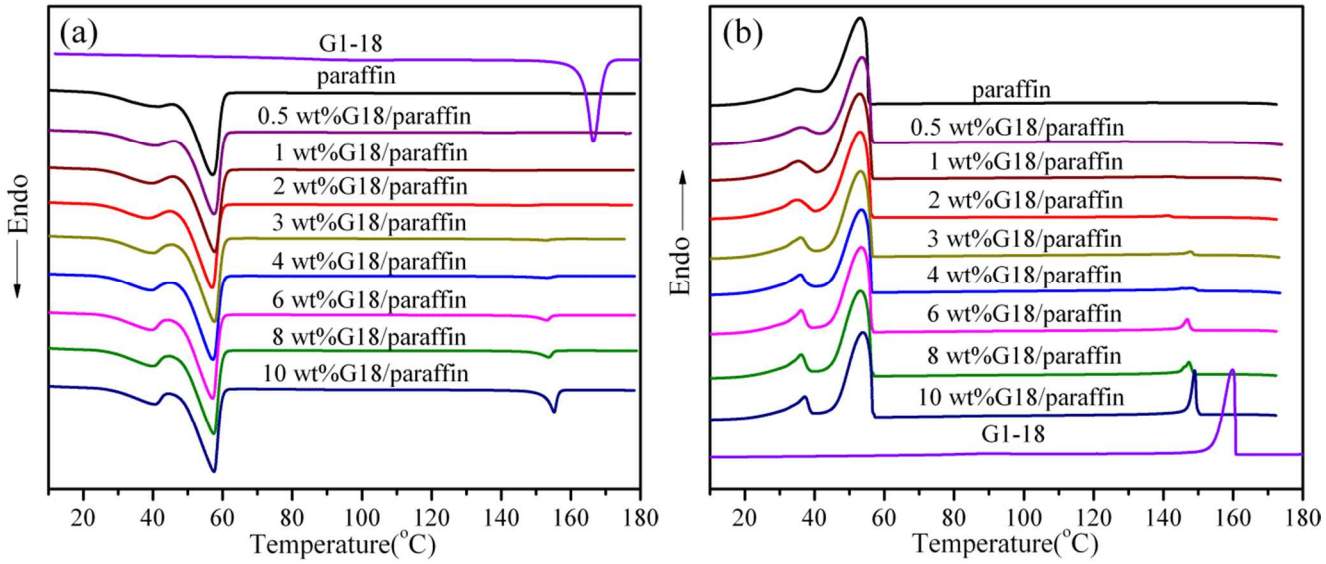

Fig.8 DSC curves of G18/paraffin composites during heating process (a) and cooling process (b).

The thermal properties of the composite G18/paraffin with different mass ratio of G18 including melting temperature of paraffin (T_m), observed melting latent heat (ΔH_m^{obs}), theoretical melting latent heat (ΔH_m^{The}), gel-sol transition temperature (T_{GS}), freezing temperature (T_f), observed freezing latent heat (ΔH_f^{obs}), theoretical freezing latent heat (ΔH_f^{The}), sol-gel transition temperature (T_{SG}) are summarized in Table 1. As seen from Table 1, compared with that of the pure paraffin, there are no differences for phase transition temperatures (T_m and T_f) of the G18/paraffin, showing that G18 has no effect on the phase transition temperature of paraffin. As can be seen in Fig.9, the T_{GS} of composite G18/paraffin increased sharply with the increase of mass fraction of G18, then increased only a little when mass fraction of G18 exceeds approximately 3 wt%. The results were coincident with the results from tube-testing method suggesting that the network was strong enough to immobilize most of the paraffin at this concentration. Therefore, 3 wt% was selected as the proper adding amount of G18. Meantime, the ΔH_m^{obs} and ΔH_f^{obs} were consistent with the theoretical value based on the mass ratio of the paraffin in the composites (See Table 1). For example, the ΔH_m^{obs} and ΔH_m^{The} of 3 wt% G18/paraffin was 184.6 J g^{-1} and 183.6 J g^{-1}, respectively. These results suggesting that both the paraffin and G18/paraffin composites exhibit similar thermal characteristics, because there was no chemical reaction between the PCMs and gelators in the preparation of G18/paraffin. Moreover, the comparison of latent heat of G18/paraffin prepared in present study with that of the different composite PCMs in literature was also given in Table 2. Based on the data in this table, it can remarkably be noted that G18/paraffin composite PCMs exhibit higher latent heat than that of other composite PCMs. This result showed that G18/paraffin composite PCM has an important potential for the application of energy storage.

The multicycle DSC scans were performed to investigate the working reliability of G18/paraffin composites during a long-term phase change process. Fig.10 shows that the DSC curves of 3 wt% G18/paraffin before and after 50 thermal cycling. From the DSC curves, phase change temperatures for melting and freezing of composite PCM before cycling were determined at 58.7 and 52.0 °C, respectively. After 50 thermal cycling, phase change temperatures for melting and freezing of composite PCM changed to 58.3 and 52.6 °C, respectively. The latent heat of fusion varied from 186.9 to 181.7 J g^{-1}, while the latent heat of freezing was changed from 187.6 to 186.9 J g^{-1}. The phase change temperature and latent heat of composite PCM only varied slightly, suggesting that the composite PCM could always maintain the stable phase change temperatures and enthalpies over the multicycle phase transitions. Therefore, the prepared form-stable composite PCM have a high working reliability to perform the energy storage-release repetitiously at an almost stable temperature.

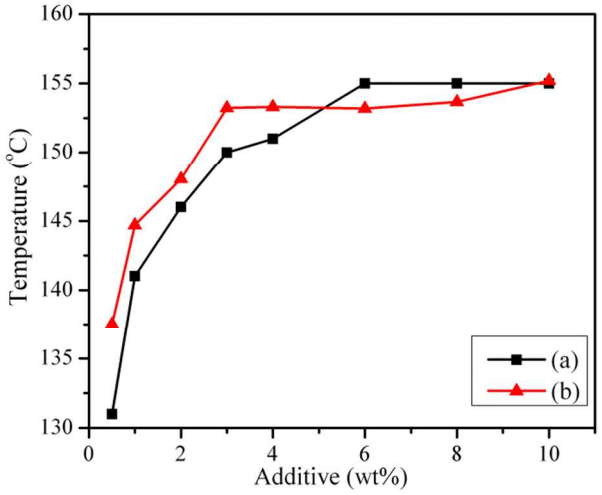

Fig.9 Relationship between the T_{GS} of G18/paraffin and the amount of G18 additive from tube-testing method (a) and DSC (b).

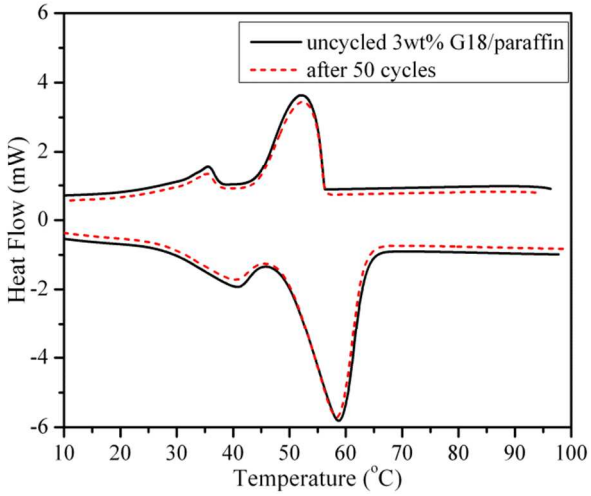

Fig.10 DSC curves of the 3 wt% G18/paraffin composite before and after thermal cycling.

Table 1 The thermal characteristics of paraffin and G18/paraffin.

	Melting				Freezing			
	T_m (°C)[a]	ΔH_m^{obs} (J g^{-1})[a]	ΔH_m^{The} (J g^{-1})[b]	T_{GS} (°C)[a]	T_f (°C)[a]	ΔH_f^{obs} (J g^{-1})[a]	ΔH_f^{The} (J g^{-1})[b]	T_{SG} (°C)[a]
paraffin	57.2	189.3	189.3	---	53.0	184.4	184.4	---
0.5 wt%G18/paraffin	57.5	173.1	188.4	137.5	53.5	172.1	183.5	129.4
1 wt%G18/paraffin	57.7	210.0	187.4	144.7	52.9	202.1	182.6	142.0
2 wt%G18/paraffin	57.0	191.6	185.5	148.0	53.0	186.2	180.7	141.1
3 wt%G18/paraffin	57.6	184.6	183.6	153.2	53.6	180.7	178.9	147.7

4 wt%G18/paraffin	57.2	184.0	181.7	153.3	53.4	177.1	177.0	147.5
6 wt%G18/paraffin	57.1	182.0	177.9	153.2	53.4	176.4	173.3	146.9
8 wt%G18/paraffin	57.5	188.1	174.6	153.7	53.1	181.7	170.0	147.3
10 wt%G18/paraffin	57.5	177.0	170.4	155.2	53.8	170.0	166.0	149.0

[a] Evaluated by DSC during the second heating process at a rate of 5 °C min^{-1} under nitrogen atmosphere.

[b] Calculated by multiplying the weight percentage of paraffin in the composite PCM by the melting or freezing enthalpies of pure paraffin.

Table 2 Comparison of thermal properties of the composite prepared with that of some FSPCMs in literatures.

FSPCM	Mass ratio	T_m (°C)[a]	T_f (°C)[b]	ΔH_m (J g^{-1})[c]	Reference
SEBS/paraffin	10/90	54.5	49.1	158.5	Q. Zhang et al.[70]
EPDM/paraffin	50/50	56.4	48.8	85.0	G. Song et al.[71]
HNT/paraffin	30/70	57.2	54.2	112.4	J. Zhang et al.[72]
HDPE/paraffin	23/77	55.7	45.2	162.2	A. Sarı et al.[73]
GO/paraffin	48.3/51.7	53.57	44.59	63.7	M. Mehrali et al.[74]
G18/paraffin	3/97	57.6	53.6	183.6	Present study
G18/paraffin	10/90	57.5	53.8	170.4	Present study

[a] Melting temperature of paraffin. [b] Freezing temperature of paraffin. [c] Melting latent heat of FSPCMs.

Rheology measurement

To examine the phase transition behavior and shape stability of materials, the G18/paraffin was characterized by rheological measurements. The storage modulus (G′) is an important parameter which characterizes the strength of gels and can estimate the degree of resistance that PCMs gels against mechanical disturbance. On the other hand, the loss modulus (G″) measures the tendency of a material to flow under stress.

In Fig.11a, the storage modulus and loss modulus of 3 wt% G18/paraffin composite were shown at four different temperatures, namely, 100, 140, 145 and 150 °C for the applied frequency range 0.1 - 100 rad s^{-1}. It is apparent from the figure that both the G′ and G″ were parallel to the frequency axis and G′ > G″ at 100 °C and 140 °C, which characterizing the system in the gel state. At 145 °C, the composite behaved as a sol (G″ > G′) for the low frequency region (below 2.4 rad s^{-1}) and above that frequency the system behaved as a gel (G′ > G″). Finally at 150 °C, the composite behaved completely as a sol (G″ > G′). These results were consistent with the results from "tube-testing method" and DSC (Fig.11b). Fig.11c shows the effect of temperature on storage modulus and loss modulus of 3 wt% G18/paraffin composites at a heating rate of 2 °C min^{-1}. To deeply investigate phase change behavior of G18/paraffin, we can divide the different changing tendencies of G′ and G″ into several segments.[67] It can be seen that two peaks of G′ and G″at around 39 °C and 57 °C agreed well with the transition temperature of composites on DSC (Fig.11b), due to a solid-solid phase transition and solid-liquid transition of the paraffin component. However, with temperature increasing gradually above 57 °C, both G′ and G″ decreased because paraffin underwent a solid-liquid phase transition, but G′ remained larger than G″ and the value kept nearly invariant up to 118 °C, implies that paraffin can be packaged in the network of G18 even above its melting point and the composite PCMs remains gel state. We denominate this solid-like gel with higher modulus as hard gel. With the increase of temperature, both G′ and G″ began to decrease steadily, but still G′ > G″, in the temperature range of 118 to 147 °C, suggesting the trend of losing solid-like characters for G18/paraffin composite PCMs. This gel with lower modulus was denominated as soft gel. A crossover point of G′ and G″ traces was found at around 147 °C, which was the symbol of gel-sol transition for rheological measurement, after that G″ would be larger than G′, the whole system presents a viscous-dominant behavior.[75-77]

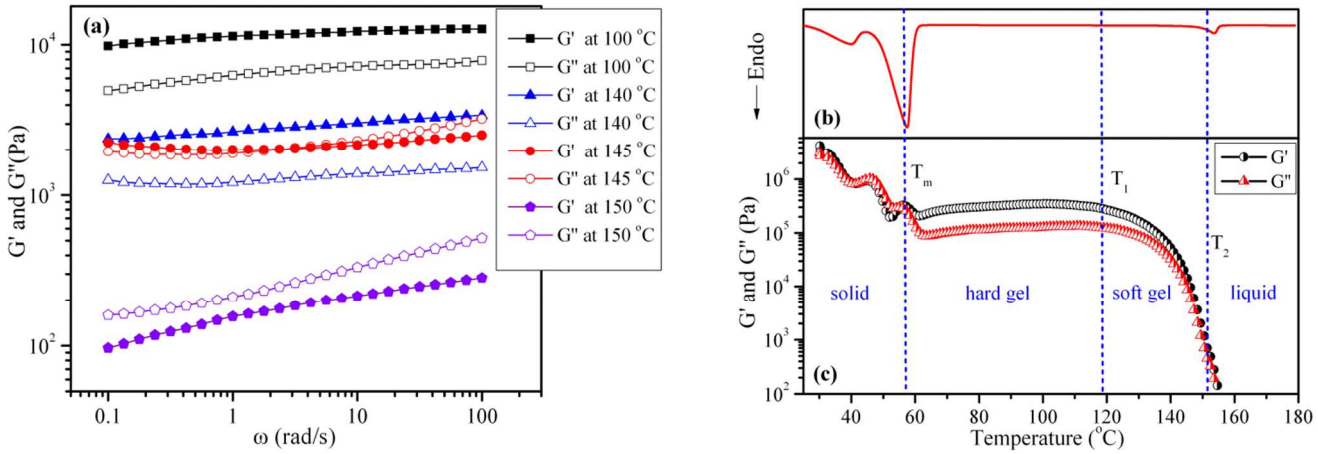

Fig.11 (a) Frequency dependence of G′ (solid symbols) and G″ (open symbols) for 3 wt% G18/paraffin composite at indicated temperature. Condition: 0.05% strain. (b) Temperature dependence of storage modulus (G′) and loss modulus (G″) for 3 wt% G18/paraffin composite at 30 °C to 160 °C. Condition: 0.05% strain, 1 rad s^{-1} frequency and 2 °C min^{-1} heating rate. (c) DSC curves of 3 wt% G18/paraffin composite during heating process.

The temperature at which G′ and G″ began to decrease was considered as transition temperature from hard gel to soft gel and was denoted as T_1, and the critical temperature that G′ equaled to G″ was denoted as T_2. With reference to Fig.12, with the increase of mass percentage of G18 in the composites, both T_1 and T_2 shifted to higher temperatures. Moreover, G′ increased along with the increase of mass fraction of gelator G18, indicating that higher concentration of gelator in PCMs tend to form more stable gels.

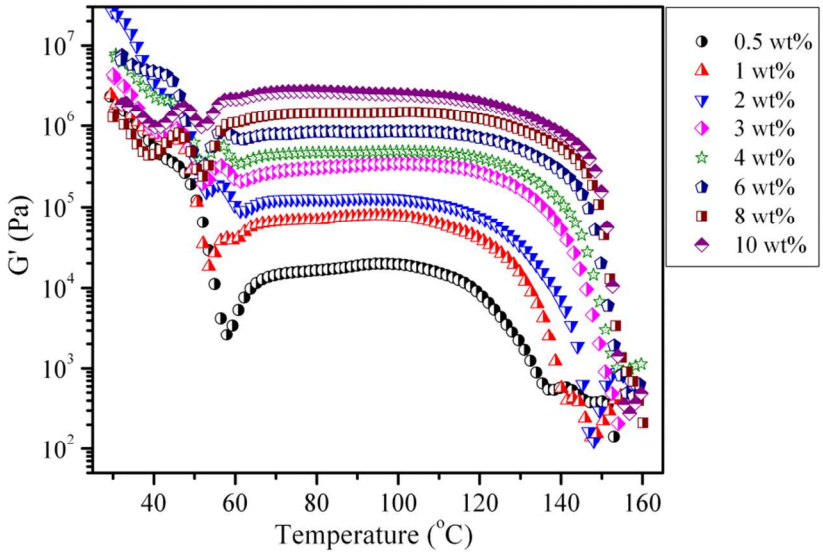

Fig.12 Temperature dependence of storage modulus for G18/paraffin composite at different mass fraction from 30 °C to 160 °C. Condition: 0.05% strain, 1 rad s^{-1} frequency and 2 °C min^{-1} heating rate.

Frequency sweeps were conducted at low strain (0.05%), well within the linear region. Testing temperature was 70 °C, at which the solid-liquid PCMs occurred phase transition. Consisted with the Fig.13, it can be seen that G18/paraffin examples exhibit weak frequency dependence from 0.1 to 100 rad s^{-1}, and the elastic modulus G′ remained larger than the viscous modulus G″, and there was almost no crossover. The value of G′ also increased with the increase of mass percentage of G18 in the composites. These dynamic mechanical results showing that the composite G18/paraffin are in a gel state, i.e., the paraffin was trapped by gel fibrillate network as solid-liquid phase transition occurred, which resulted in FSPCMs.

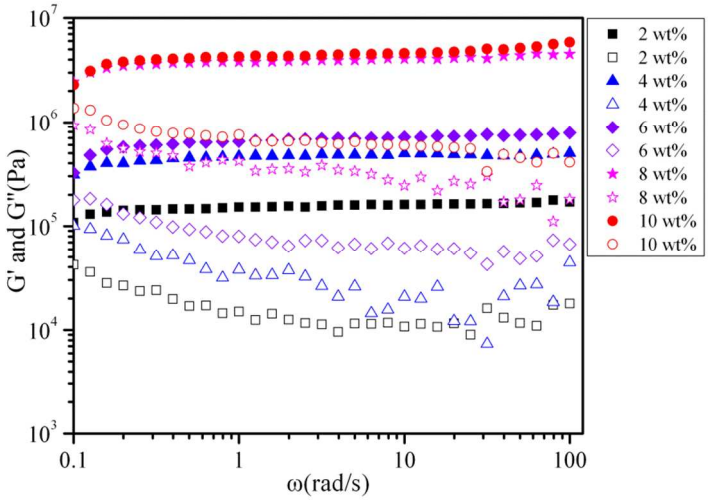

Fig.13 Frequency dependence of G′ (solid symbols) and G″ (open symbols) for G18/paraffin composite PCMs of different concentration of G18. Condition: 0.05% strain, 70 °C.

According to the analyses above, we charted a "phase diagram" of G18/paraffin FSPCMs as Fig.14. The vertical axis represents temperature while the horizontal axis represents the content of G18 in the composites. T_m, T_1, T_2 were determined by the former rheological analysis of G18/paraffin composites. As shown in Fig.14, when the temperature was below about 57 °C, the melting point of paraffin, both pure paraffin and G18/paraffin composites were in solid state. With temperature increased above the melting point, the pure paraffin melted into liquid, while the composites formed hard gel. In this condition, the paraffin was trapped by gel fibrillate network of G18. When the temperature further increased above T_1, the composites turned into soft gel and its rigidity decreased. In this case, the gel network started to collapse but the shape of samples was partially maintained, and the overall state was still similar to solid rather than liquid. With temperature increased above T_2, the composites became fluid, losing its shape stability completely. Meantime, with the increase of G18 content, both T_1 and T_2 of the G18/paraffin FSPCMs shifted to higher temperatures. However, when the adding amount of G18 was more than 3 wt% or so, the T_1 and T_2 basically reached a plateau, so the 3 wt% was considered as the proper adding amount of G18 to keep the G18/paraffin composite stable.

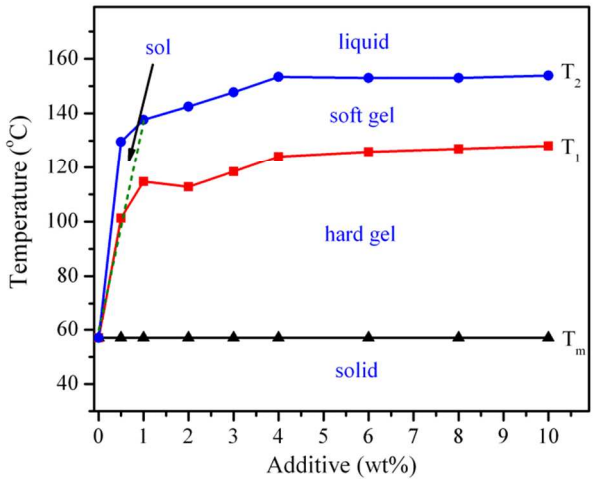

Fig.14 "Phase diagram" of G18/paraffin composite during heating.

Conclusions

In this work, a novel FSPCMs (Gm/paraffin (m = 8, 10, 12, 14, 16, 18)) which owning high heat storage density and excellent thermal stability were successfully prepared by introducing 4, 4′-diaminodiphenylmethane-based gelators into paraffin. FT-IR, POM, WAXD and SEM measurement suggested that the paraffin acted as latent heat storage material while gelators served as supporting material, and the paraffin was restricted by three-dimensional netted structural of gelators to avoid leakage even above their melting point. The G18/paraffin composites exhibited high heat storage density and excellent thermal stability from the DSC and rheology measurement. The mass percentage of paraffin can reach 97 wt% without obvious leakage of paraffin above the melting point and the composites can keep their shapes in a long range of temperature due to the excellent supporting ability of gel network from G18. As a result, the T_{GS} of 3 wt% G18/paraffin FSPCMs was 150 °C, which was well above the melting point of paraffin, and values of the melting and freezing enthalpies were 184.6 and 180.7 J g^{-1}, making the G18/paraffin composite an effective and promising material to store or release thermal energy in practical application. The research on Gm/paraffin composite provided a new method for FSPCMs, and meanwhile broadened the application field of gelators.

Acknowledgments

This research was financially supported by the National Nature Science Foundation of China (51373148), the Opening Project of Key Laboratory of Polymeric Materials and Application Technology of Hunan Province (PMAT201401).

Notes and references

1 B. Zalba, J. M. Marín, L. F. Cabeza and H. Mehling, *Appl. Therm. Eng.*, 2003, **23**: 251-283.
2 A. Sarı and A. Biçer, *Sol. Energy Mater. Sol. Cells*, 2012, **101**, 114-122.
3 A. Najjar and A. Hasan, *Energy Convers. Manage.*, 2008, 49, 3338-3342.

4 A. Sharma, V. V. Tyagi, C. R. Chen and D. Buddhi, *Renew. Sust. Energy Rev.*, 2009, **13**, 318-345.
5 A. Jamekhorshid, S. M. Sadrameli and M. Farid, *Renew. Sust. Energy Rev.*, 2014, **31**, 531-542.
6 Y. Tian and C. Y. Zhao, *Appl. Energy*, 2013, **104**, 538-553.
7 C. Chen, L. Wang and Y. Huang, *Chem. Eng. J.*, 2009, **150**, 269-274.
8 Z. Zhang and X. Fang, *Energy Convers. Manage.*, 2006, **47**, 303-310.
9 X. Wang, E. Lu and W. Lin, *Energy Convers. Manage*. 2000, **41**, 135-144.
10 10 K. Chen, X. Yu, C. Tian and J. Wang, *Energy Convers. Manage.*, 2014, **77**, 13-21.
11 Y. Jiang and E. Ding, G. Li, *Polymer*, 2002, **43**, 117-122.
12 M. Delgado, A. Lázaro, J. Mazo and B. Zalba, *Renew. Sust. Energy Rev.*, 2012, **16**, 253-273.
13 P. B. Salunkhe and P. S. Shembekar, *Renew. Sust. Energy Rev.,* 2012, **16**, 5603-5616.
14 H. Fauzi, H. S. Metselaar, T. M. I. Mahlia and M. Silakhori, *Solar Energy*, 2014, **102**, 333-337.
15 N. Zhu, Z. Ma and S. Wang, *Energy Convers. Manage.,* 2009, **50**, 3169-3181.
16 Y. Wang, T. D. Xia, H. Zheng and H. X. Feng, *Energy and Buildings*, 2011, **43**, 2365-2370.
17 C. Wang, L. Feng, W. Li, J. Zheng, W. Tian and X. Li, *Sol. Energy Mater. Sol. Cells*, 2012, **105**, 21-26.
18 M. Xiao, B. Feng and K. Gong, *Energy Convers. Manage.*, 2002, **43**, 103-108.
19 M. M. Farid, A. M. Khudhair, S. A. K. Razack and S. Al-Hallaj, *Energy Convers. Manage.*, 2004, **45**, 1597-1615.
20 A. M. Khudhair and M. M. Farid, *Energy Convers. Manage.*, 2004, **45**, 263-275.
21 D. Rozanna, T. G. Chuah, A. Salmiah, T. S. Y. Choong and M. Sa'ari, *Int. J. Green Energy*, 2005, **1**, 495-513.
22 S. D. Sharma and K. Sagara, *Int. J. Green Energy*, 2005, **2**, 1-56.
23 V. V. Tyagi, D. Buddhi, *Renew. Sust. Energy Rev.*, 2007, **11**, 1146-1166.
24 V. V. Tyagi, S. C. Kaushik, S. K. Tyagi and T. Akiyama, *Renew. Sust. Energy Rev.*, 2011, **15**, 1373-1391.
25 M. Kenisarin and K. Mahkamov, *Renew. Sust. Energy Rev.*, 2007, **11**, 1913-1965.
26 M. M. Kenisarin, *Renew. Sust. Energy Rev.*, 2010, **14**, 955-970.
27 A. Pasupathy, R. Velraj and R. V. Seeniraj, *Renew. Sust. Energy Rev.*, 2008, **12**, 39-64.
28 F. Agyenim, N. Hewitt, P. Eames and M. Smyth, *Renew. Sust. Energy Rev.*, 2010, **14**, 615-628.
29 R. Baetens, B. P. Jelle and A. Gustavsen, *Energy and Buildings*, 2010, **42**, 1361-1368.
30 C. Y. Zhao and G. H. Zhang, *Renew. Sust. Energy Rev.*, 2011, **15**, 3813-3832.
31 L. F. Cabeza, A. Castell, C. Barreneche, A. de Gracia and A. I. Fernández, *Renew. Sust. Energy Rev.*, 2011, **15**, 1675-1695.
32 F. Kuznik, D. David, K. Johannes and J. J. Roux, *Renew. Sust. Energy Rev.*, 2011, **15**, 379-391.
33 L. Fan and J. M. Khodadadi, *Renew. Sust. Energy Rev.*, 2011, **15**, 24-46.
34 V. A. A. Raj and R. Velraj, *Renew. Sust. Energy Rev.*, 2010, **14**, 2819-2829.
35 J. L. Zeng, J. Zhang, Y. Y. Liu, Z. X. Cao, Z. H. Zhang, F. Xu and L. X. Sun, *J. Therm. Anal. Calorim.*, 2008, **91**, 455-461.
36 J. A. Molefi, A. S. Luyt, I. Krupa, *Thermochim. Acta*, 2010, **500**, 88-92.
37 G. Fang, H. Li, Z. Chen and X. Liu, *J. Hazard. Mater.*, 2010, **181**, 1004-1009.
38 M. Silakhori, H. S. C. Metselaar, T. M. I. Mahlia, H. Fauzi, S. Baradaran and M. S. Naghavi, Energy Convers. Manage., 2014, **80**, 491-497.
39 Y. Wang, T. D. Xia, H. X. Feng and H. Zhang, *Renew. Ener.*, 2011, **36**, 1814-1820.
40 C. Alkan and A. Sari, *Sol. Energy*, 2008, **82**, 118-124.
41 F. Chen and M. P. Wolcott, *Eur. Polym. J.*, 2014, **52**, 44-52.
42 X. Wang, Q. Guo, J. Wang, Y. Zhong, L. Wang, X. Wei and L. Liu, *Renew. Energy*, 2013, **60**, 506-509.
43 Y. Cai, Q. Wei, F. Huang and W. Gao, *Appl. Energy*, 2008, **85**, 765-775.
44 M. J. Hato and A. S. Luyt, *J. Appl. Polym. Sci.*, 2007, **104**, 2225-2236.
45 C. Alkan, K. Kaya and A. Sari, *J. Polym. Environ.*, 2009, **17**, 254-258.
46 A. Sari, A. Karaipekli and C. Alkan, *Chem. Eng. J.*, 2009, **155**, 899-904.
47 D. Sun, L. Wang and C. Li, *Mater. Lett.*, 2013, **108**, 247-249.
48 A. Karaipekli and A. Sari, *Sol. Energy*, 2009, **83**, 323-332.
49 S. Karaman, A. Karaipekli, A. Sari and A. Biçer, *Sol. Energy Mater. Sol. Cells*, 2011, **95**, 1647-1653.
50 A. Sari and A. Karaipekli, *Sol. Energy Mater. Sol. Cells*, 2009, **93**, 571-576.
51 Q. Cao and P. Liu, *Eur. Polym. J.*, 2006, **42**, 2931-2939.
52 J. C. Su and P. S. Liu, *Energy Convers. Manage.*, 2006, **47**, 3185-3191.
53 Q. Meng and J. Hu, *Sol. Energy Mater. Sol. Cells*, 2008, **92**, 1260-1268.
54 L. Bayés-García, L. Ventolà, R. Cordobilla, R. Benages, T. Calvet and M. A. Cuevas-Diarte, *Sol. Energy Mater. Sol. Cells*, 2010, **94**, 1235-1240.
55 A. Sari, C. Alkan, A. Karaipekli and O. Uzun, *Sol. Energy*, 2009, **83**, 1757-1763.
56 J. Li, P. Xue, H. He, W. Ding and J. Han, *Energy and Buildings*, 2009, **41**, 871-880.
57 B. Tang, J. Cui, Y. Wang, C. Jia and S. Zhang, *Sol. Energy*, 2013, **97**, 484-492.
58 G. Fang, H. Li and X. Liu, *Mater. Chem. Phys.*, 2010, **122**, 533-536.
59 W. Wang, X. Yang, Y. Fang and J. Ding, *Appl. Energy*, 2009, **86**, 170-174.
60 P. Dastidar, S. Okabe, K. Nakano, K. Iida, M. Miyata, N. Tohnai and M. Shibayama, *Chem. Mater.*, 2005, **17**, 741-748.
61 X. Zhang, P. Deng, R. Feng and J. Song, *Sol. Energy Mater. Sol. Cells*, 2011, **95**, 1213-1218.
62 T. Tian, J. Song, L. Niu and R. Feng, *Thermochim. Acta*, 2013, **554**, 54-58.
63 J. He, B. Yan, B. Yu, R. Bao, X. Wang and Y. Wang, *J. Colloid Interface Sci.*, 2007, **316**, 825-830.
64 H. Svobodová, Z. Wimmer and E. Kolehmainen, *J. Colloid Interface Sci.*, 2011, **361**, 587-593.
65 S. Grassi, E. Carretti, L. Dei, C. W. Branham, B. Kahr and R. G. Weiss, *New J. Chem.*, 2011,35, 445-452.
66 R. Schmidt, F. B. Adam, M. Michel, M. Schmutz, G. Decher and P. J. Mésini, *Tetrahedron Lett.*, 2003, **44**, 3171-3174.
67 H. Yui, H. Minamikawa, R. Danev, K. Nagayama, S. Kamiya and T. Shimizu, *Langmuir*, 2008, **24**,709-713.
68 J. L. Li, X. Y. Liu, C. S. Strom and J. Y. Xiong, *Adv. Mater.*, 2006, **18**, 2574-2578.
69 Y. Xiong, Q. Liu, H. Wang and Y. Yang, *J. Colloid Interface Sci.*, 2008, **318**, 496-500.
70 Q. Zhang, Y. Zhao and J. Feng, *Sol. Energy Mater. Sol. Cells*, 2013, **118**, 54-60.
71 G. Song, S. Ma, G. Tang, Z. Yin and X. Wang, *Energy*, 2010, **35**, 2179-2183.
72 J. Zhang, X. Zhang, Y. Wan, D. Mei and B. Zhang, *Solar Energy*, 2012, **86**, 1142-1148.
73 A. Sarı, Energy Convers. Manage., 2004, **45**, 2033-2042.
74 M. Mehrali, S. T. Latibari, M. Mehrali, H. S. C. Metselaar and M. Silakhori, *Energy Convers. Manage.*, 2013, **67**, 275–282.
75 A. I. Van Den Bulcke, B. Bogdanov, N. De Rooze, E. H. Schacht, M. Cornelissen and H. Berghmans, *Biomacromolecules*, 2000, **1**, 31-38.
76 D. Dasgupta, S. Manna, A. Garai, A. Dawn, C. Rochas, J. M. Guenet and A. K. Nandi, *Macromolecules*, 2008, **41**, 779-787.
77 A. Garai and A. K. Nandi, *J. Polym. Sci., Part B: Polym. Phys.*, 2008, **46**, 28-40.

Table of contents entry：

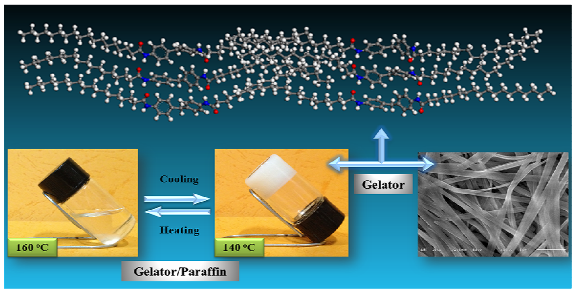

Gelator/paraffin composites as a novel FSPCM supported by gelator network with high heat storage density and excellent thermal stability.